Journal of Applied Fluid Mechanics, Vol. 11, No. 4, pp. 1059-1071, 2018.
Available online at www.jafmonline.net, ISSN 1735-3572, EISSN 1735-3645.
DOI: 10.29252/jafm.11.04.28038

On the Optimization of the Species Separation in an Inclined Darcy-Brinkman Porous Cavity under the Effect of an External Magnetic Field

A. Rtibi[1†], M. Hasnaoui[2] and A. Amahmid[2]

[1] *Mohammed V University, Faculty of Sciences, MSME, Rabat, Morocco*
[2] *Cadi Ayyad University, Faculty of Sciences Semlalia, LMFE, Marrakesh, Morocco*

†*Corresponding Author Email: a.rtibi@uca.ac.ma*

(Received May 23, 2017; accepted January 13, 2018)

ABSTRACT

An investigation is conducted to study analytically and numerically the effect of a magnetic field on the species separation induced by the combined effects of convection and Soret phenomenon in an inclined porous cavity saturated by an electrically conductive binary mixture and provided with four impermeable walls. The long sides of the cavity are subject to uniform heat flux while its short ends are adiabatic. Uniform magnetic field is applied perpendicularly to the heated walls. The mixture satisfies the Boussinesq approximation and the porous medium, modeled according to Darcy-Brinkman's law, is assumed homogeneous and isotropic .The relevant parameters for the problem are the thermal Rayleigh number (R_T = 1 to 10^6), the Lewis number (Le = 10), the inclination angle of the cavity (θ = 0º to 180), the separation parameter (φ = 0.5), the Darcy number (Da = 10^{-5} to 10^3), the Hartmann number (Ha = 0 to 100) and the aspect ratio of the cavity (A_r = 12). The limiting cases (Darcy and pure fluid media) are recovered in this study. Optimum conditions leading to maximum separation of species are determined while varying the governing parameters in their respective ranges. Results show that the magnetic field can enhance the species separation in cases where the optimal coupling between thermosolutal diffusion and convection is not achieved in its absence. On the other hand, in cases where this optimal coupling is reached in the absence of the magnetic field, the application of the latter destroys the separation of species.

Keywords: Darcy-Brinkman porous medium; Soret effect; Magnetic field; Separation of species; Analytical and numerical study.

NOMENCLATURE

A_r	aspect ratio of the porous matrix, L'/H	(u,v)	dimensionless velocities, $((u'H'/a, v'H'/a)$
D	mass diffusivity of species	(x,y)	dimensionless coordinates, $(x'/H', y'/H')$
D^T	thermosolutal diffusion coefficient	**Greek symbols**	
D_{eff}	effective mass diffusivity, $\varepsilon' D$	α	thermal diffusivity
Da	effective Darcy number, $\mu_e K/\mu H'^2$	β_s	solutal expansion coefficient
g	gravitational acceleration	β_T	thermal expansion coefficient
H	height of the enclosure	γ	electrical conductivity
Ha	Hartmann number, $B\sqrt{\gamma K/\mu}$	ε	porosity of the porous medium
K	permeability of the porous medium	ν	kinematic viscosity of the fluid
L	width of the porous layer	ρ	density of the fluid mixture
Le	Lewis number, α/D	λ	thermal conductivity
Nu	Nusselt number	ϕ	separation parameter, $\beta_s \Delta S'/\beta_T \Delta T$
q	constant heat flux per unit area	ψ	dimensionless stream function, ψ'/α
R_T	thermal Darcy-Rayleigh number, $g\beta_T K \Delta T' H'/(\alpha\nu)$	$(\rho C)_F$	heat capacity of the fluid mixture
S	dimensionless solute concentration,		

	$(S' - S'_0) / \Delta S$
S_0	reference solute concentration (at $x = y = 0$)
$\Delta S'$	characteristic solute concentration, $-D_T S'_0 (1 - S'_0) \Delta T' / D_{eff}$
Sh	Sherwood number
t	dimensionless time, $t'a / \sigma L'^z$
T	dimensionless temperature, $\left(T' - T'_0\right) / \Delta T$
T_0	reference temperature (at $x = y = 0$)
ΔT	characteristic temperature, $H'q' / \lambda$
$(\rho C)_S$	heat capacity of the saturated porous medium
σ	heat capacity ratio, $(\rho C)_F / (\rho C)_S$
ε	normalized porosity, ε' / σ

Superscript

'	dimensional variable

Subscripts

max	maximum value
min	minimum value
0	a reference state
S	solutal
T	thermal

1. INTRODUCTION

Thermosolutal natural convection is induced by combined effects of heat and mass transfer under a gravity field (Clusius *et al.* 1939; Furry *et al.* 1939; De Groot 1942). When the mass diffusion due to temperature gradient occurs, the thermosolutal convection is named thermo-diffusion convection. This phenomenon is behind the occurrence of concentration stratification in an initially homogeneous composition of mixtures (Ahadi *et al.* 2013; Jaber *et al.* 2006). Owing to this phenomenon, thermosolutal separation is used for measurements of the diffusion coefficient, especially in liquid metals and fluids of industrial interest. Therefore, the more separation improvement in the experimental device, the more accurate and reliable data are obtained (Bou-Ali *et al.* 2003; Platten *et al.* 2006). Recently, the subject of separation improvement in fluid mixtures has received an increasing attention. In this frame, some researcher teams (Shevtsova 2010) planned to carry experiments on board of a spacecraft on orbit (i.e. under microgravity conditions) in order to minimize convection effect which usually disturbs the separation process. However, it is possible to improve the species separation by taking into account the convection phenomenon but by optimizing the coupling between the latter and the thermosolutal diffusion, in such a way that the regulation of the convection velocity achieves the optimum coupling. In this way, Lorenz *et al.* (1959) proposed to fill the cavity with a porous medium. In such a packed cavity, an optimal permeability of the porous medium ensures a maximum of separation. The so-called packed thermal diffusion cell described by these authors has been used intensively to perform experiments on varieties of ionic and organic mixtures (Costesèque *et al.* 1982; Costesèque *et al.* 1994, 2002). Some authors proposed to incline the thermogravitational column from the vertical position (Platten *et al.* 2003). By tilting a cell heated from above or from below, Elhajjar *et al.* (2010) showed that the separation can be significantly increased for an optimal value of the tilt angle of inclination. Another suggestion proposed by Bennacer *et al.* (2009) was to partition the domain in three parts using solid horizontal walls with porous media in the central part. They demonstrated that the increase in the curvature of the cylindrical annulus allows a higher species separation due to the non-symmetrical temperature profile. All above experimented techniques aim to overcome working with cells of a few mm thickness (Platten *et al.* 2004; Marcoux *et al.* 2007). Yacine *et al.* (2016) studied analytically and numerically Soret-driven convection in a horizontal porous layer saturated by a binary fluid and subjected to uniform cross heat fluxes. The fluid flow was driven by the combined buoyancy effect due to temperature and induced mass fraction variations through a binary water ethanol mixture. Good agreement was observed between the analytical and numerical results concerning the species separation obtained for a unicellular flow. The Soret separation process is improved by two control parameters, the heat flux density imposed on the horizontal walls of the cell and the ratio of the heat flux density imposed on the vertical walls to that on the horizontal ones. The influence of the heat flux density ratio, on the transient regime (relaxation time) was also investigated numerically. The separation phenomenpn in ternary mixture n-dodecane, isobutylbenzene, and tetralin was studied analytically and numerically by Larabi *et al.* (2016) in order to corroborate the experimental measurements of the thermal diffusion coefficients obtained in microgravity in the international space station. The authors show that it is possible to quantify and to optimize the species separation for ternary mixtures. In a recent paper published by Alain Martin *et al.* (2018), the separation process was analyzed both numerically and experimentally in a mixture of dimethyl sulfoxide in phosphate buffered saline. Their results confirm that the effect of thermodiffusion must be considered to hand processes of biological fluid mixtures because the existence of a thermal gradient could improve the efficiency of the separation process in micro devices.

In the case of an electrically conducting fluid, numerous investigations were devoted to understand the effect of a magnetic field on heat and mass transfer induced in binary mixtures with Soret diffusion. For instance, Pal *et al.* (2012) studied analytically the influence of Soret effect on magneto-hydro-dynamic (MHD) mixed oscillatory convection over a vertical surface in a porous medium. The authors reported that the local Sherwood number decreases with the increase of the Soret number. Raju *et al.* (2008) examined the effect of a weak magnetic field on the species separation of species in a binary mixture under a fully developed natural convection between two

inclined plates. They concluded that the rarer and lighter component of the binary mixture increases in the central part of the plates by decreasing the strength of the magnetic field, but a reverse action prevails near the plates. Rao *et al.* (2012) studied hydromagnetic boundary layer flow over a vertical plate in the presence of Soret effect. All the governing parameters showed a significant effect on the fluid flow and heat and mass transfer characteristics. The onset of thermomagnetic convection in ferrofluids was exanimate by Sprenger *et al.* (2013), using a linear stability analysis. They found that thermodiffusion with a positive sign of the Soret coefficient precipitates the onset of convection, whereas negative coefficients suppress convection at all. Rtibi *et al.* (2014) studied numerically and analytically the effect of a transverse magnetic field on buoyancy-driven convection in an inclined rectangular Darcy porous cavity, saturated with an electrically conducting mixture. Their results show that the magnetic buoyancy force has a stabilizing effect on the system since it leads to a reduction of the flow intensity and heat transfer. However, it could engender an increase or a reduction of the mass transfer depending on the values of the Hartmann number, the inclination angle of the cavity and the separation ratio. Ben Sassi *et al*. (2017) investigated numerically the effect of thermodiffusion on solute segregation during the growth of semiconductor materials in the case of pure thermal convection corresponding to dilute alloys. Their results indicate that variations in the sign of the Soret parameter can lead to diametrically opposite behaviors, while an increase in the intensity of the thermal convection generally leads to a mitigation of the effects induced by thermodiffusion.

In the present study, we suggest to apply a transversal magnetic field normal to the long sides of an inclined rectangular porous cavity, uniformly heated from these sides and having impermeable and adiabatic ends. The porous medium is modeled using the Darcy-Brinkman extended model with the Boussinesq approximation. The study focuses mainly on the improvement of species separation by seeking optimum coupling effects between porosity (via the Darcy number), inclination angle of the cavity and the magnetic field.

2. MATHEMATICAL FORMULATION

The studied configuration is sketched in Fig. 1. It consists of a two-dimensional and homogeneous inclined porous layer of height H and width L'. The short walls of the layer are adiabatic and impermeable while its long inclined walls are subject to uniform fluxes of heat, q′, and to a transversal magnetic field, $\vec{B}$.

The porous medium is assumed isotropic and sparsely or well packed such that the convective flow is modelled using the extended Darcy-Brinkman model and the binary fluid that saturates the porous medium is modelled as a Boussinesq incompressible fluid obeying the approximation

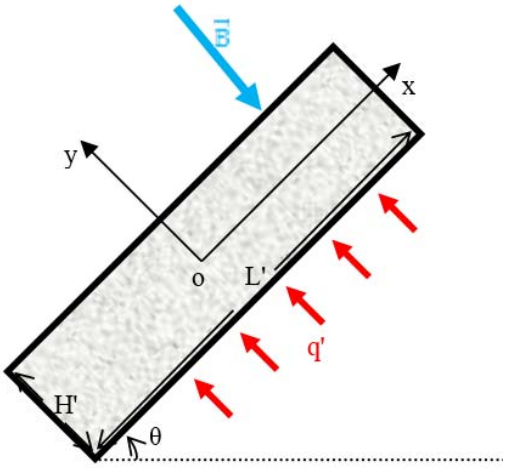

Fig. 1. Schematic diagram of the physical model.

$\rho = \rho_0\left(1-\beta_T\left(T'-T_0'\right)-\beta_S\left(S'-S_0'\right)\right)$. Assuming constant properties and taking into account the Soret effect (the Dufour effect is neglected, which is the case in liquid mixtures), the dimensionless governing equations describing the conservation of momentum, energy and species in the saturated porous medium are:

$$\nabla^2\psi + Ha^2\frac{\partial u}{\partial y} = -R_T\left(\cos\theta\frac{\partial}{\partial x}-\sin\theta\frac{\partial}{\partial y}\right)\left(T+\varphi S\right)+$$

$$u\frac{\partial T}{\partial x}+v\frac{\partial T}{\partial y}=\nabla^2 T \qquad (2)$$

$$u\frac{\partial S}{\partial x}+v\frac{\partial S}{\partial y}=\frac{1}{Le^2}\left(\nabla^2 S-\nabla^2 T\right) \qquad (3)$$

$$u=\frac{\partial\psi}{\partial y},\quad v=-\frac{\partial\psi}{\partial x} \qquad (4)$$

In the above equations, ψ, T and S are the dimensionless stream function, temperature and solute concentration, respectively. The following boundary conditions are associated to the governing equations

$$\left.\begin{aligned} y=\pm 1/2:\frac{\partial\psi}{\partial y}=\psi=0 and\frac{\partial T}{\partial y}=\frac{\partial S}{\partial y}=-1\\ x=\pm A_r/2:\frac{\partial\psi}{\partial x}=\psi=0 and\frac{\partial T}{\partial x}=\frac{\partial S}{\partial x}=0\end{aligned}\right\} \qquad (5)$$

The present problem is seen to be governed by seven dimensionless parameters which are the separation parameter, φ, the Hartmann number, Ha, the thermal Darcy-Rayleigh number, R_T ,the effective Darcy number, Da, the Lewis number, Le, the cavity aspect ratio, A_r, and the inclination of the cavity, θ. These parameters are defined as follow:

$$\left.\begin{aligned} &\varphi=-\beta_s S_0'\left(1-S_0'\right)D_T/\beta_T D_{eff},\\ &Da=\mu_e K/\mu H'^2, \qquad Ha=B\sqrt{\gamma K/\mu}\\ &R_T=g\beta_T\Delta T' K H'/\alpha\nu, \qquad Le=\alpha/D_{eff}\\ &and \qquad A_r=L'/H'\end{aligned}\right\} \qquad (6)$$

where $D_{eff} = D\varepsilon$ is the effective mass diffusivity and D and D_T stay respectively for mass diffusivity and thermosolutal diffusion coefficient.

3. NUMERICAL METHOD

The numerical solution of the full governing equations is based on a second order accurate finite-difference method. An iterative procedure is performed using the Alternate Direction Implicit (A.D.I) method to solve Eqs. (1) to (3). The stream function field was determined from Eq. (4) using the point successive-over-relaxation method. The grid distribution is uniform per zone and carefully chosen so that a fine sub-grid is constructed near the confining walls to capture the steep velocity, temperature and concentration gradients. Further details on the numerical method and its validation can be found in the studies by Amahmid *et al.* (1999) and Bourich *et al.* (2005). Based on the sensitivity analysis of the grid, all numerical calculations were performed with a relatively fine grid consisting of 121×101 nodes. This grid allows reproducing the analytical results with insignificant differences as seen in the following paragraphs.

4. ANALYTICAL SOLUTION

Illustrative streamlines, isotherms and iso-solutes lines, obtained numerically and presented in Figs. 2 for $R_T = 200$, $Le = 10$, $\varphi = 0.5$, $Da = 0.01$, $A_r = 12$ and $\theta = 163^\circ$ and 90° justify clearly the approximation of the parallel flow based on the fact that the flow is parallel to the long sides in the core region of the enclosure, while the temperature and the concentration are linearly stratified in the x-direction. Consequently, provided that the aspect ratio of the porous layer is large enough $(A_r >> 1)$, the present problem can be significantly simplified to allow the development of and analytical solution based on the parallel flow approximation (Bourich *et al.* 2005; Comarck 1974 and many others).

The approximations used are $\psi(x,y) = \psi(y)$, $T(x,y) = C_T x + \theta_T(y)$ and $S(x,y) = C_s x + \theta_s(y)$. The parameters C_T and C_s stay respectively for unknown constant temperature and concentration gradients in the x direction. They are determined by imposing zero heat and mass net fluxes across any transversal section of the cavity " Alavyoon (1993) ", which leads to the following integral forms:

$$\left.\begin{aligned}\int_{-\frac{1}{2}}^{\frac{1}{2}}\left(uT-\frac{\partial T}{\partial x}\right)dy = 0\\ \int_{-\frac{1}{2}}^{\frac{1}{2}}\left(uS-\frac{1}{Le}\left(\frac{\partial S}{\partial x}-\frac{\partial T}{\partial x}\right)\right)dy = 0\end{aligned}\right\} \quad (7)$$

Combination of the above approximations with the steady-state Eqs. (1)-(4), leads to the following system of ordinary differential equations

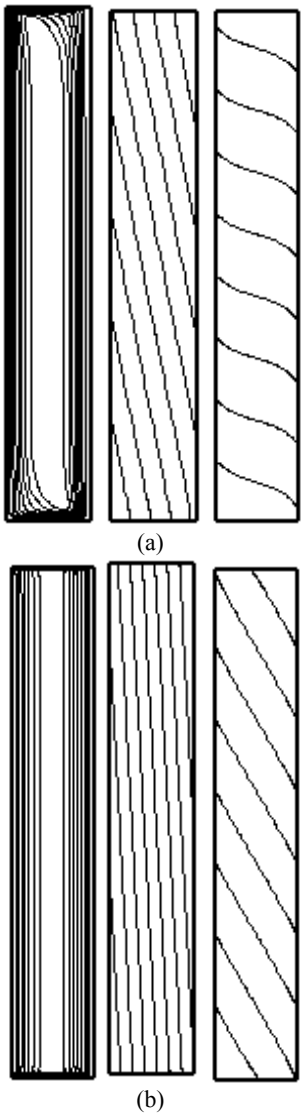

Fig. 2. Streamlines, isotherms and iso-solutes (from left to right) for *Da* = 0.01, φ = 0.5, *Le* = 10, R_T = 200*:* (a) (θ,*Ha*) = (163°,1) *and* (b) (θ,*Ha*) = (90°,30).

$$\frac{d^4\psi}{dy^4} - \frac{1}{D_m}\frac{d^2\psi}{dy^2} + \frac{\omega^2}{D_m}\psi - \frac{G\omega^2}{D_m} = 0 \quad (8)$$

$$\frac{d^2\theta_T}{dy^2} = C_T\frac{d\psi}{dy} \quad (9)$$

$$\frac{d^2\theta_s}{dy^2} = \left(C_T + C_S Le\right)\frac{d\psi}{dy} \quad (10)$$

The boundary conditions at $y = \pm 1/2$ are such that

$$\psi = \frac{d\psi}{dy} = 0 \text{ and } \frac{d\theta_T}{dy} = \frac{d\theta_s}{dy} = -1 \quad (11)$$

where:

$\left(1+Ha^2\right)Da = D_m$,

$\omega^2\left(1+Ha^2\right)=R_T\left[C_T+\varphi\left(C_T+C_S Le\right)\right]\sin\theta$ and

$G\omega^2\left(1+Ha^2\right)=R_T\left[\left(C_T+\varphi C_S\right)\cos\theta+\left(1+\varphi\right)\sin\theta\right]$

The analytical solution predicted by the parallel flow approximation depends on the signs of the following expressions:

ω^2 , $\Omega_p^2=\left(1/2D_m\right)\left(1+\sqrt{1-4D_m\omega^2}\right)$,

$\left(1/4\,D_m{}^2\right)\left(1-4D_m\omega^2\right)$,

and $\Omega_m^2=\left(1/2D_m\right)\left(1-\sqrt{1-4D_m\omega^2}\right)$. Hence, different cases emerge and should be discussed.

4.1 Case 1: $0\le 4D_m\omega^2\le 1$

Under this condition, the solution of the problem is obtained as

$$\psi\left(y\right)=G-B_p\Omega_p\cosh\left(\Omega_p y\right)-B_m\Omega_m\cosh\left(\Omega_m y\right) \tag{12}$$

$$T\left(x,y\right)=C_T x+\left(C_T G-1\right)y-C_T \left(B_P\sinh\left(\Omega_p y\right)+B_m\sinh\left(\Omega_m y\right)\right) \tag{13}$$

$$S\left(x,y\right)=C_S x+\left(\left(C_T+LeC_S\right)G-1\right)y -\left(C_T+LeC_S\right)\left(B_P\sinh\left(\Omega_p y\right)+B_m\sinh\left(\Omega_m y\right)\right) \tag{14}$$

where:

$B_p=A_1 G/\Omega_p$

$B_m=A_2 G/\Omega_m$

$\Omega_p=\sqrt{1/2D_m}\sqrt{1+\sqrt{1-4D_m\omega^2}}$

$\Omega_m=\sqrt{1/2D_m}\sqrt{1-\sqrt{1-4D_m\omega^2}}$

$A_1=\dfrac{A_{11}}{A_{12}}$

$A_2=\dfrac{A_{22}}{A_{12}}$

$A_{11}=-\Omega_m\sinh\left(\Omega_m/2\right)$

$A_{22}=\Omega_p\sinh\left(\Omega_p/2\right)$

$A_{12}=\Omega_p\sinh\left(\Omega_p/2\right)\cosh\left(\Omega_m/2\right)-\Omega_m\sinh\left(\Omega_m/2\right)\cosh\left(\Omega_p/2\right)$

The analytical expressions of C_T and C_S are determined via Eq. (8) as follows

$C_T=\left(1-C_T G\right)\beta_1+C_T\left(\beta_2+\beta_3\beta_4\right)$

$C_s=C_T+Le\left[\left[1-\left(C_T+LeC_s\right)G\right]\beta_1+\left[C_T+LeC_s\right]\left(\beta_2+\beta_3\beta_4\right)\right]$

where

$\beta_1=\alpha_{2p}B_p+\alpha_{2m}B_m$

$\beta_2=\alpha_{1p}B_p^2+\alpha_{1m}B_m^2$

$\beta_3=\dfrac{2B_pB_m\left(\Omega_p^2+\Omega_m^2\right)}{\left(\Omega_p^2-\Omega_m^2\right)}$

$\beta_4=\left[\Omega_p\sinh\left(\Omega_m/2\right)\cosh\left(\Omega_p/2\right)-\Omega_m\sinh\left(\Omega_p/2\right)\cosh\left(\Omega_m/2\right)\right]$

$\alpha_{1p}=\left(\Omega_p/2\right)\left(\sinh\left(\Omega_p\right)-\Omega_p\right)$,

$\alpha_{1m}=\left(\Omega_m/2\right)\left(\sinh\left(\Omega_m\right)-\Omega_m\right)$

$\alpha_{2p}=\Omega_p\cosh\left(\Omega_p/2\right)-2\sinh\left(\Omega_p/2\right)$,

$\alpha_{2m}=\Omega_m\cosh\left(\Omega_m/2\right)-2\sinh\left(\Omega_m/2\right)$

4.2 Case2: $\omega^2<0$

For this case, the solution of the problem turns to:

$$\psi\left(y\right)=G+A_1\cosh\left(\Omega_p y\right)+A_2\cos\left(\Omega_m y\right) \tag{15}$$

$$T\left(x,y\right)=C_T x+\left(C_T G-1\right)y+C_T\left(\left(A_1/\Omega_p\right)\sinh\left(\Omega_p y\right)+\left(A_2/\Omega_m\right)\sin\left(\Omega_m y\right)\right) \tag{16}$$

$$S\left(x,y\right)=C_S x+\left(\left(C_T+LeC_S\right)G-1\right)y+\left(C_T+LeC_S\right)\left(A_1/\Omega_p\right)\sinh\left(\Omega_p y\right)+\left(C_T+LeC_S\right)\left(A_2/\Omega_m\right)\sin\left(\Omega_m y\right) \tag{17}$$

where:

$A_1=\dfrac{A_{11}}{A_{12}}$

$A_2=\dfrac{A_{22}}{A_{12}}$

$A_{11}=-G\Omega_m\sin\left(\Omega_m/2\right)$

$A_{22}=-G\Omega_p\sinh\left(\Omega_p/2\right)$

$A_{12}=\Omega_p\sinh\left(\Omega_p/2\right)\cos\left(\Omega_m/2\right)+\Omega_m\sin\left(\Omega_m/2\right)\cosh\left(\Omega_p/2\right)$

$\Omega_p=\sqrt{1/2D_m}\sqrt{1+\sqrt{1-4D_m\omega^2}}$

$\Omega_m=\sqrt{1/2D_m}\sqrt{-1+\sqrt{1-4D_m\omega^2}}$

$$C_T = \left(C_T G - 1\right)\gamma_1 + C_T\gamma_2$$

$$C_S = C_T + Le\left[\left[\left(C_T + LeC_s\right)G - 1\right]\gamma_1 + \left(C_T + LeC_s\right)\gamma_2\right]$$

$$\gamma_1 = \left(A_1\Omega_p I_1 - A_2\Omega_m I_5\right)$$

$$\gamma_2 = \left(A_1^2 I_2 - A_2^2 I_4\right) + A_1 A_2 I_3\left(\Omega_p/\Omega_m - \Omega_m/\Omega_p\right)$$

The I_i (i = 1, ..,5) parameters in the above expressions are obtained as:

$$I_1 = \left(1/\Omega_p\right)\left[\cosh\left(\Omega_p/2\right) - \left(2/\Omega_p\right)\sinh\left(\Omega_p/2\right)\right]$$

$$I_2 = \left(1/2\Omega_p\right)\left[\sinh\left(\Omega_p\right) - \Omega_p\right]$$

$$I_3 = \left(2\Big/\left(\Omega_p^2 + \Omega_m^2\right)\right)\left[\Omega_p\cosh\left(\Omega_p/2\right)\sin\left(\Omega_m/2\right) - \Omega_m\sinh\left(\Omega_p/2\right)\cos\left(\Omega_m/2\right)\right]$$

$$I_4 = \left(1/2\Omega_m\right)\left[\Omega_m - \sin\left(\Omega_m\right)\right]$$

$$I_5 = \left(1/\Omega_m\right)\left[\left(2/\Omega_m\right)\sin\left(\Omega_m/2\right) - \cos\left(\Omega_m/2\right)\right]$$

4.3 Case3: $4D_m\omega^2 \geq 1$

For this last case, the analytical solution is obtained as follows:

$$\psi\left(y\right) = G + A_1\cosh\left(\Omega_p y\right)\cos\left(\Omega_m y\right) + A_2\sinh\left(\Omega_p y\right)\sin\left(\Omega_m y\right) \tag{18}$$

$$T\left(x,y\right) = C_T x + \left(C_T G - 1\right)y + C_T\left(A_1 I_1\left(\Omega_p,\Omega_m,y\right) + \left(A_2 + A_1\Omega_m/\Omega_p\right)I_4\left(\Omega_p,\Omega_m,y\right)\right) \tag{19}$$

$$S\left(x,y\right) = C_S x + \left(\left(C_T + LeC_S\right)G - 1\right)y + \left(C_T + LeC_S\right)A_1 I_1\left(\Omega_p,\Omega_m,y\right) + \left(C_T + LeC_S\right)\left(A_2 + A_1\Omega_m/\Omega_p\right)I_4\left(\Omega_p,\Omega_m,y\right) \tag{20}$$

where:

$$A_1 = \frac{A_{11}}{A_{12}}$$

$$A_2 = \frac{A_{22}}{A_{12}}$$

$$A_{11} = -G\left(\Omega_p\cosh\left(\Omega_p/2\right)\sin\left(\Omega_m/2\right) + \Omega_m\sinh\left(\Omega_p/2\right)\cos\left(\Omega_m/2\right)\right)$$

$$A_{22} = G\left(\Omega_p\sinh\left(\Omega_p/2\right)\cos\left(\Omega_m/2\right) - \Omega_m\cosh\left(\Omega_p/2\right)\sin\left(\Omega_m/2\right)\right)$$

$$A_{12} = \Omega_p\sin\left(\Omega_m/2\right)\cos\left(\Omega_m/2\right) + \Omega_m\sinh\left(\Omega_p/2\right)\cosh\left(\Omega_p/2\right)$$

$$\Omega_p = \left(1/\sqrt{4D_m}\right)\sqrt{\sqrt{4D_m\omega^2} + 1}$$

$$\Omega_m = \left(1/\sqrt{4D_m}\right)\sqrt{\sqrt{4D_m\omega^2} - 1}$$

$$C_T = G + 2A_1\begin{bmatrix} I_1\left(\Omega_p,\Omega_m,1/2\right) + \left(\Omega_m/\Omega_p\right) \\ I_4\left(\Omega_p,\Omega_m,1/2\right)\end{bmatrix} + 2A_2 I_4\left(\Omega_p,\Omega_m,1/2\right) - C_T\begin{pmatrix} G^2 + A_1^2/4 \\ -A_2^2/4\end{pmatrix} - 4C_T G A_1 I_1\left(\Omega_p,\Omega_m,1/2\right) - 4C_T G\left[\left(\Omega_m/\Omega_p\right)A_1 + A_2\right]I_4\left(\Omega_p,\Omega_m,1/2\right) - C_T A_1 A_2 I_4\left(2\Omega_p,2\Omega_m,1/2\right) - C_T\left(A_1^2/2 - A_2^2/2\right)\left[I_1\left(2\Omega_p,2\Omega_m,1/2\right) + \left(\Omega_m/\Omega_p\right)I_4\begin{pmatrix}2\Omega_p, \\ 2\Omega_m,1/2\end{pmatrix}\right] - C_T\left(A_1^2/4 + A_2^2/4\right)\left[I_2\left(2\Omega_m\right) + I_3\left(2\Omega_p\right)\right]$$

$$C_S = C_T + LeG + 2LeA_1 I_1\left(\Omega_p,\Omega_m,1/2\right) + 2LeA_1\left(\Omega_m/\Omega_p\right)I_4\left(\Omega_p,\Omega_m,1/2\right) + 2LeA_2 I_4\left(\Omega_p,\Omega_m,1/2\right) - Le\left(C_T + LeC_S\right)\left(G^2 + A_1^2/4 - A_2^2/4\right) - 4Le\left(C_T + LeC_S\right)G\left[A_1 I_1\left(\Omega_p,\Omega_m,1/2\right) + \left[\left(\Omega_m/\Omega_p\right)A_1 + A_2\right]I_4\left(\Omega_p,\Omega_m,1/2\right)\right] - Le\left(C_T + LeC_S\right)A_1 A_2 I_4\left(2\Omega_p,2\Omega_m,1/2\right) - Le\left(C_T + LeC_S\right)\left(A_1^2/2 - A_2^2/2\right)\left[I_1\left(2\Omega_p,2\Omega_m,1/2\right) + \left(\Omega_m/\Omega_p\right)I_4\left(2\Omega_p,2\Omega_m,1/2\right)\right] - Le\left(C_T + LeC_S\right)\left(A_1^2/4 + A_2^2/4\right)\left[I_2\left(2\Omega_m\right) + I_3\left(2\Omega_p\right)\right]$$

Where:

$$I_1\left(\Omega_p,\Omega_m,y\right) = \left(1/\Omega_p\right)\sinh\left(\Omega_p y\right)\cos\left(\Omega_m y\right))$$

$$I_2\left(\Omega_m\right) = \left(2/\Omega_m\right)\sin\left(\Omega_m/2\right),$$

$$I_3\left(\Omega_p\right) = \left(2/\Omega_p\right)\sinh\left(\Omega_p/2\right),$$

$$I_4\left(\Omega_p,\Omega_m,y\right) = \left(1\Big/\left(\Omega_p^2 + \Omega_m^2\right)\right)\left[\Omega_p\cosh\left(\Omega_p y\right)\sin\left(\Omega_m y\right) - \Omega_m\sinh\left(\Omega_p y\right)\cos\left(\Omega_m y\right)\right]$$

5. RESULTS AND DISCUSSIONS

The species separation ΔC in a binary mixture is

defined as the difference of the mass fraction of the denser species between the end-walls (shorts walls) of the cell located at $x = A_r/2$ *and* $-A_r/2$. For a tall cavity, the species separation is given directly by the solute gradient coefficient C_S which is predicted by the analytical solution based on the parallel flow approximation. It is well known that the separation of species in a binary mixture can be improved by realizing an optimal compromise between thermo-diffusion and convection by acting on the flow intensity. The latter can be reduced by varying the permeability of the porous medium via the Darcy number, by tilting the cavity or by imposing an external magnetic field to the system. This section is devoted to study the combined effects of all these parameters on the separation of species using illustrations supported by data analysis and discussion. Results are presented in terms of evolutions of the flow intensity ψ_C in the center of the cavity and species separation ΔC of the binary mixture versus Ha and θ for $R_T = 200$ and 1000, $\varphi = 0.5$, $Le = 10$, $A_r = 12$ and different values of Da.

5.1 Effect of the Hartmann Number

The Hartmann number, Ha, is a measure of the magnetic force. It could be varied by acting on the strength of the magnetic field, by considering various working electrically conducting fluids or different porous media with different permeabilities. The effect of the Hartmann number on the profiles of the longitudinal velocity u is presented in Fig. 3 for two combinations of R_T, Da and θ. These profiles confirm the monocellular nature of the flow and show that the increase of the Hartmann number has a weakening effect on the velocities along all the cross section of the porous layer.

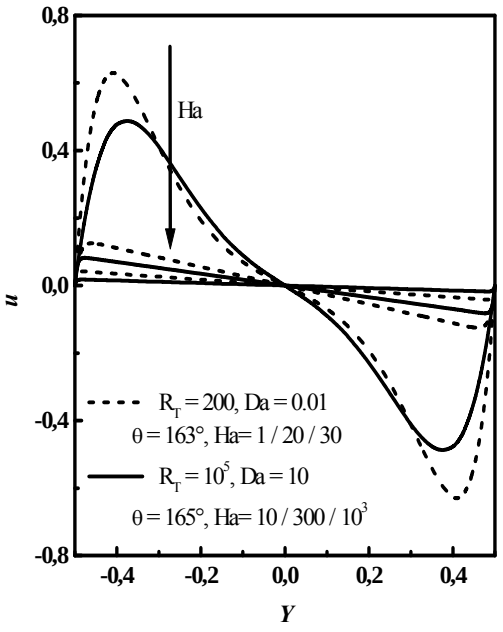

Fig. 3. Profiles of the longitudinal velocity for $Le = 10$, $\varphi = 0.5$.

The effect of the Hartmann number on the species separation, ΔC and the global intensity of the flow, ψ_C (i.e. the flow intensity measured by the stream function at the centre of the cavity), is illustrated in Figs. 4a-b for different combinations of the triplet (Da, θ, R_T). Understandably, the values selected for the parameters are those leading to an optimal separation in the absence of the magnetic field and the objective here consists to examine how the magnetic field acts on the optimum. From Fig. 4a, it is seen that the optimum value of separation remains insensitive to the increase of Ha as long as its value is lower than a threshold value Ha_c. The latter is located in the range]3, 10[and it is obviously dependent on the combination (Da, θ, R_T) Once the threshold value of Ha is reached, more increase of this parameter leads to a monotonous and drastic decrease of the species separation toward zero. In fact, the damping role of the magnetic field on convection is characterized by an important reduction of the flow intensity for sufficiently large values of this parameter as it is seen in Fig. 4b. Hence, the increase of the magnetic field intensity above some thresholds breaks up the optimum coupling and affects seriously the separation of species. The curves of Fig. 4a show that for Ha varying in the range [0, 5], the triplet $(Da, \theta, R_T) = (20, 90^\circ, 1000)$ is the least favorable to the species separation compared to the other triplets. In fact, within this range of Ha, Fig. 4b indicates that the highest values of ψ_C correspond to the triplet $(Da, \theta, R_T) = (20, 90^\circ, 1000)$; the optimum value of ψ_C leading to the maximum separation of species is just below 0.12.

For sparsely packed porous cavity $(Da = 0.01)$ and $(\varphi, Le, R_T) = (0.5, 10, 200)$ the evolution of ψ_C with Ha depends strongly on the inclination θ. In fact, for $\theta = 45^\circ$ Fig. 5b shows that the evolution of ψ_C vs. Ha is characterized first by a slow decrease for $Ha \le 0.3$, followed by a drastic decrease for $0.3 \le Ha \le 30$. Above the upper limit of the precedent range (i.e. for $Ha > 30$), ψ_C becomes insensitive to the variations of Ha. The effect of Ha is seen to be more and more attenuated by increasing the inclination angle and the range of Ha corresponding to the sharp decrease of ψ_C is more and more reduced. In addition, for inclinations above 165°, the effect of Ha becomes insignificant in the whole range of its variation. Moreover, for a given small to moderate value of Ha, ψ_C decreases by increasing θ with a decreasing rate accompanying the increase of Ha. In Fig. 5a that exemplifies the variations of ΔC versus Ha, it can be seen that, as long as $Ha \le 1$ the separation phenomenon is negligible for $\theta \le 105^\circ$. This behavior is expected since, within these ranges of

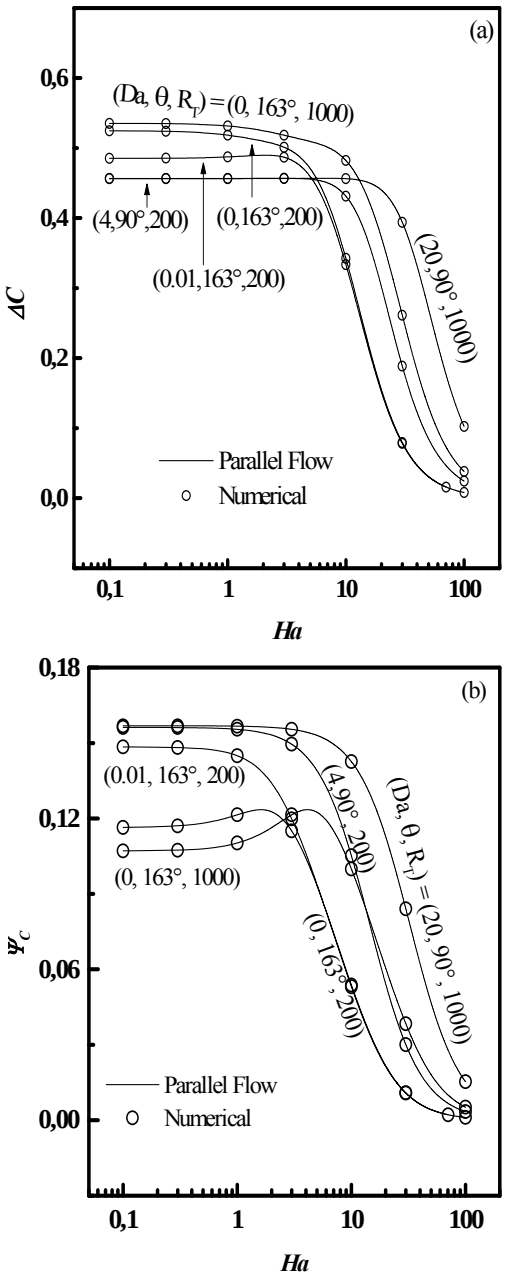

Fig. 4. Variations vs. Ha **of** ΔC **(a) and** ψ_C **(b) for** $Le = 10$ **,** $\varphi = 0.5$ **and various combinations of** Da **,** Ha **and** R_T **.**

θ and Ha, values of ψ_C are much higher than the optimal values promoting the separation of species which are around 0.1. For $\theta = 135^\circ$ and 150° and $Ha \le 1$ the values of ψ_C are respectively around 1 and 0.5 leading to weak and moderate values of ΔC. Beyond the value $Ha = 1$, $\left(i.e.\ for\ 1 < Ha \le 100\right)$, the separation undergoes an important increase (accompanying the decrease of ψ_C) towards a maximum whose value and location are nearly independent of θ varying within the range $\left[45^\circ, 105^\circ\right]$. For $\theta = 135^\circ$ and 150°, the location of the maximum of separation is slightly shifted towards smaller values of Ha by increasing θ without any significant quantitative change on the value of ΔC. For the remaining values of θ in the studied range i.e. for $\theta \ge 160^\circ$, the evolution of ΔC vs. Ha exhibits a substantial change in the behavior in comparison with the cases discussed above for the remaining inclinations. In fact, for $\theta = 165^\circ$, the separation of species is important in the range $0.1 \le Ha \le 1$ but it undergoes a sharp decrease towards zero beyond $Ha = 2$. A similar behavior is also observed for $\theta = 170^\circ$ but in favor of $\theta = 165^\circ$ in terms of separation of species. This behavior is characterized first by the constancy of ΔC for small Hartmann numbers, preluding its sharp decrease. For $\theta = 160^\circ$ and 163°, the evolution of ΔC with Ha shows an increase toward a maximum after the constancy range (the maximum is barely visible for $\theta = 163^\circ$) before undergoing a sharp decrease towards zero. For $Ha < 1$, the inclinations leading to the largest separation are $\theta = 163^\circ$ and 165°. The separation of speciesis nearly constant in this range of Ha (ΔC is around 0.49). Above $Ha = 12$, the maximum of separation is induced by inclinations within the range $\left[45^\circ, 105^\circ\right]$ with a non-significant change of its value. For the intermediate range of Ha, $3 < Ha < 12$, the maximum of separation is obtained for one of the inclinations $\theta = 160^\circ, 150^\circ$ and 135°; depending on the considered sub-interval of Ha within this range. More precisely, the maximum value of ΔC, which is about 0.49, is observed around $Ha = 4.02 / (7.4) / (10.5)$ for $\theta = 160^\circ / \left(150^\circ\right) / \left(135^\circ\right)$. The location of the maximum of ΔC remains unchanged and it is obtained around Ha = 14.5 for θ varying in the range $\left[45^\circ, 105^\circ\right]$.

The iso-solutes illustrated in Figs. 6a-c for $(\theta, Ha) = \left(163^\circ, 1\right)$, $\left(163^\circ, 30\right)$ and $\left(90^\circ, 14.75\right)$ show clearly that the separation of species depends strongly on the combined effects of θ and Ha when the values of the remaining parameters remain unchanged. The examination of Fig. 6 shows that the combination (163°, 30) corresponding to Fig. 6b is far from ensuring a separation sought while the remaining combinations lead to a good separation of species. It is to note from the iso-solutes of Fig. 6 that the optimal separation doesn't match with the most distorted iso-solutes; this observation is in accordance with the attenuation of the separation phenomenon in the presence of a strong convection. In summary, the results presented reveal that, depending on the inclination θ, there exists a specific range of Ha promoting the separation. In this range, the optimum coupling between

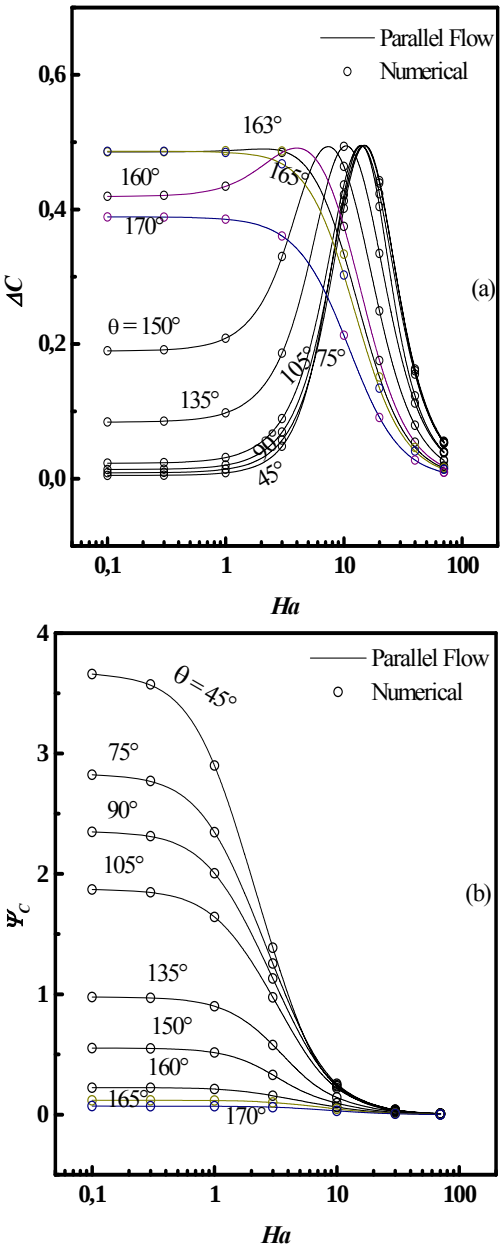

Fig. 5. Effect of Ha **on** ΔC **and** ψ_C **for** $Le = 10$, $\varphi = 0.5$, $R_T = 200$ **and** $Da = 0.01$.

thermodiffusion and convection is attained by sufficiently weakening the role of convection in such a way that the flow intensity ψ_C falls around 0.1 under the conjugate effect of θ and Ha. In Fig. 6a and 6c, where the separation of species is achieved, $\psi_C = 0.144$ and 0.134 (values of $O(10^{-1})$ while in Fig. 6b, $\psi_C = 0.010$; intensity ten times lower than that ensuring an effective separation which leads to a vanishing of the latter.

In the case of pure fluid medium, limit recovered with the Darcy-Brinkman model for $Da = 10$, the examination of Figs. 7a-b obtained with $R_T = 10^5$, indicates that the behaviors of ΔC and ψ_C in their evolutions vs. Ha are characterized by some

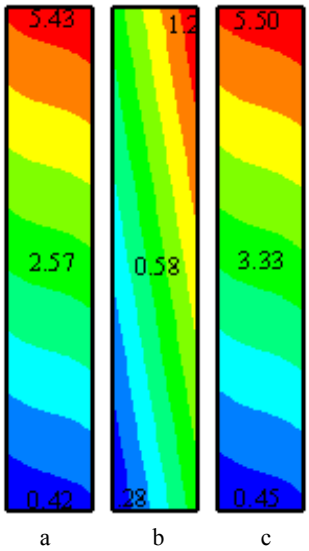

Fig. 6. Iso-concentration lines for $Le = 10$, $\varphi = 0.5$, $R_T = 200$ **and** $Da = 0.01$**: (a)** $(\theta, Ha) = (163°, 1)$**, (b)** $(\theta, Ha) = (163°, 30)$ **and (c)** $(\theta, Ha) = (90°, 14.75)$.

qualitative similarities with those described respectively in Figs. 5a-b for a pure Darcy medium. Quantitatively, the curves of Fig. 7a show that the maximum values reached by ΔC are nearly unchanged for the same inclination in comparison with those obtained in the case of Darcy medium. However, the locations of these maximums are strongly shifted towards larger values of Ha for θ varying in the range $[45° - 160°]$. In fact, the important increase of the flow intensity caused by $R_T = 10^5$ in the absence of the magnetic field requires higher values of Ha to bring the flow intensity to values of $O(10^{-1})$ ensuring an optimum separation of the species (Fig. 7b). The threshold value of Ha below which the inclinations $\theta = 163°$ *and* 165° ensure a better separation compared to the remaining inclinations is importantly increased to reach a value of Ha around 60 for $(Da, R_T) = (10, 10^5)$. These results show the important role that could be played by the magnetic force to counteract the promoting role (in terms of flow intensity) of the buoyancy force in favor of the separation of species.

5.2 Effect of the Cavity Inclination

The effect of the inclination on the flow intensity and species separation is illustrated in Figs. 8a-b for Darcy medium with $(Da, R_T) = (0.01, 200)$ and in Figs. 9a-b for fluid medium for $(Da, R_T) = (10, 10^5)$. The analysis is conducted for $\varphi = 0.5$, $Le = 10$ and various Ha. In the case of

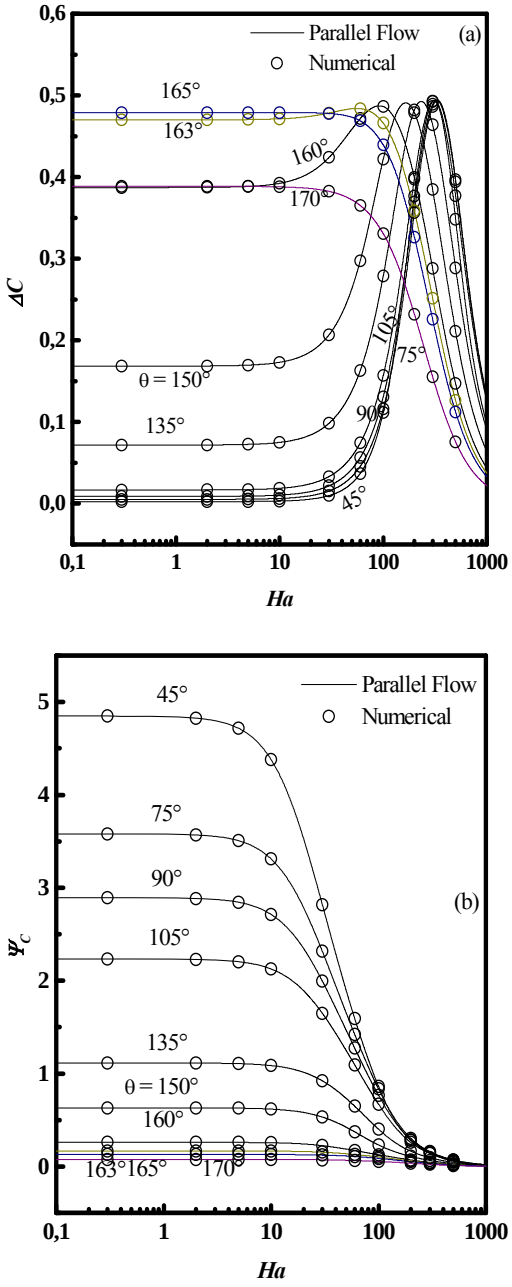

Fig. 7. Variations vs. Ha **of** ΔC **(a) and** ψ_C **(b) for** $Le=10$, $\varphi=0.5$, $R_T=10^5$, $Da=10$ **and various values of** θ.

the porous medium, Fig. 8a indicates that ΔC reaches its maximum for an inclination around 90° for $Ha=30$. By increasing/decreasing the inclination of the cavity from its vertical position $\left(\theta=90^\circ\right)$, toward $\theta=180^\circ/\left(0^\circ\right)$ which corresponds to a cavity heated from above/(below), the separation of species undergoes a continuous decrease toward 0 (value obtained for 0° and 180°). This means that, at $Ha=30$, the coupling between thermodiffusion and convection is optimal for $\theta=90^\circ$ though it leads to a moderate separation since the maximum value of ΔC reached for this inclination is around 0.27. Any increase or decrease of θ from this value leads to a destruction of this quasi-optimal coupling by deviating the flow intensity from the optimum value. The separation of species vanishing for $\theta=180^\circ$ and 0° is explained differently for both inclinations. In fact, for $\theta=180^\circ$, the cavity is horizontal and heated from above. The stability of the equilibrium solution is more reinforced by the positive separation ratio $\left(\varphi=0.5>0\right)$ and the fluid remains at rest. For this inclination, the fluid motionlessness is obviously maintained for all values of Ha. For the other inclination limit $\left(\theta=0^\circ\right)$ and $Ha=30$, the cavity is horizontal and heated from below. The absence of the flow circulation is attributed to the fact that Rayleigh number is still below the critical value required for the onset of convection, which leads to $\Delta C=0$. For $\theta=0^\circ$ and the remaining values of Ha, the value of ΔC depends on either the generated flow intensity is close or far from the optimum one which is of $O\left(10^{-1}\right)$ as mentioned before. More precisely, $\Delta C\left(Ha=4\right)<\Delta C\left(Ha=10\right)<\Delta C_{\max}$ and these results are corroborated by the corresponding flow intensity in Fig. 8b. In addition, $\Delta C\left(Ha=0\right)=\Delta C\left(Ha=1\right)=0$ since the corresponding ψ_C are larger than the required order ensuring the maximum separation of the species. The examination of Fig. 8a shows that the inclinations leading to $\Delta C_{\max}$ depends strongly on Ha. In fact, this maximum $\left(\Delta C_{\max}=0.49\right)$ is reached for θ around $160^\circ/\left(164^\circ\right)$ for $Ha=4/\left(Ha=0\ and\ 1\right)$. Above these thresholds inclinations, ΔC decreases drastically and vanishes for $\theta=180^\circ$, as the system falls in the diffusive regime. Finally, for $Ha=10$, the separation of species behaves differently in comparison with the other values of Ha. In fact, for this value of Hartmann number, the evolution of ΔC vs. θ indicates that the maximum value of $\Delta C\left(\Delta C_{\max}\approx 0.49\right)$ is reached for two inclinations, $\theta_1=10^\circ$ and $\left(\theta_2=139^\circ\right)$. For θ varying between θ_1 and θ_2, $\Delta C_{\min}$ is about 0.4, which means that the maximum relative variation of ΔC doesn't exceed 18.3%.

In the case of pure fluid medium, recovered by the Brinkman model and illustrated here with $Da=10$, the examination of Figs. 9a-b shows that the evolutions of ψ_C and ΔC vs. θ are qualitatively similar to those described in Figs. 8a-b for a Darcy medium. Here, $Ha=0$ and 1 lead to identical qualitative and quantitative behaviors while for the d processes of biological fluid mixtures because th

Ha induces a small quantitative effect on ΔC and a perceptible quantitative effect on ψ_C mainly for inclinations below 90° (see Figs. 8a and 8b). The behavior discussed before for the porous medium with $Ha = 30$ is reproduced here for the fluid medium with $Ha = 500$ but with a noticeable increase of ΔC_{max} which attains 0.4 (to be compared with 0.27 of Fig. 8a). The inclinations leading to the maximum of ΔC are 165°, 160° and 80° respectively for $Ha = 1{,}100$ and 500.

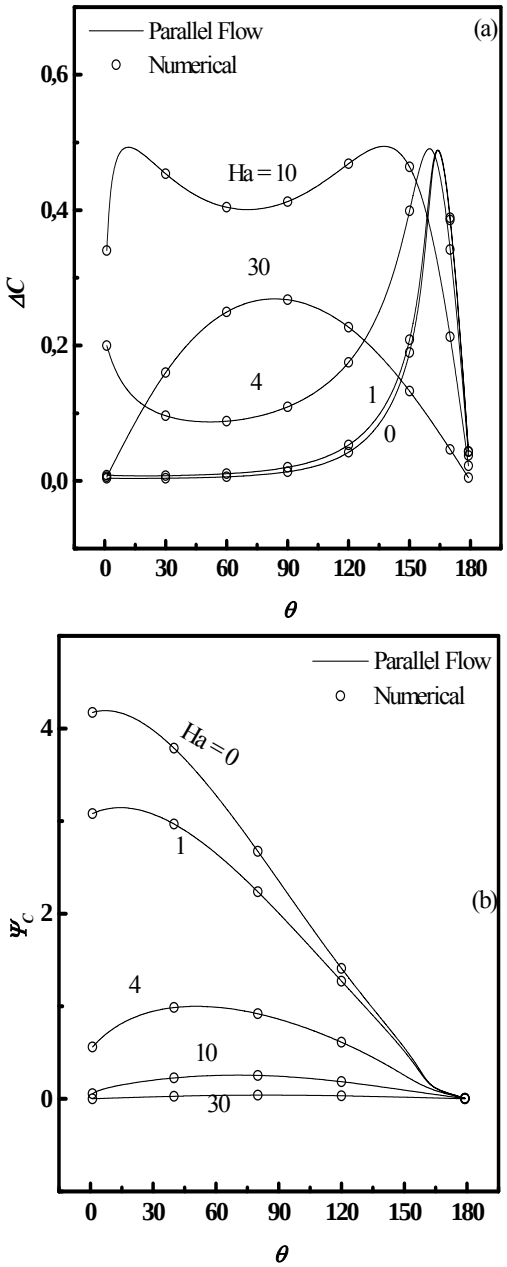

Fig. 8: Variations vs. θ of ΔC (a) and ψ_C (b) for $Le = 10$, $\varphi = 0.5$, $R_T = 200$, $Da = 0.01$ and various values of *Ha*.

For $Ha = 300$, Fig. 9a indicates that a relatively important separation is obtained in a wide range of

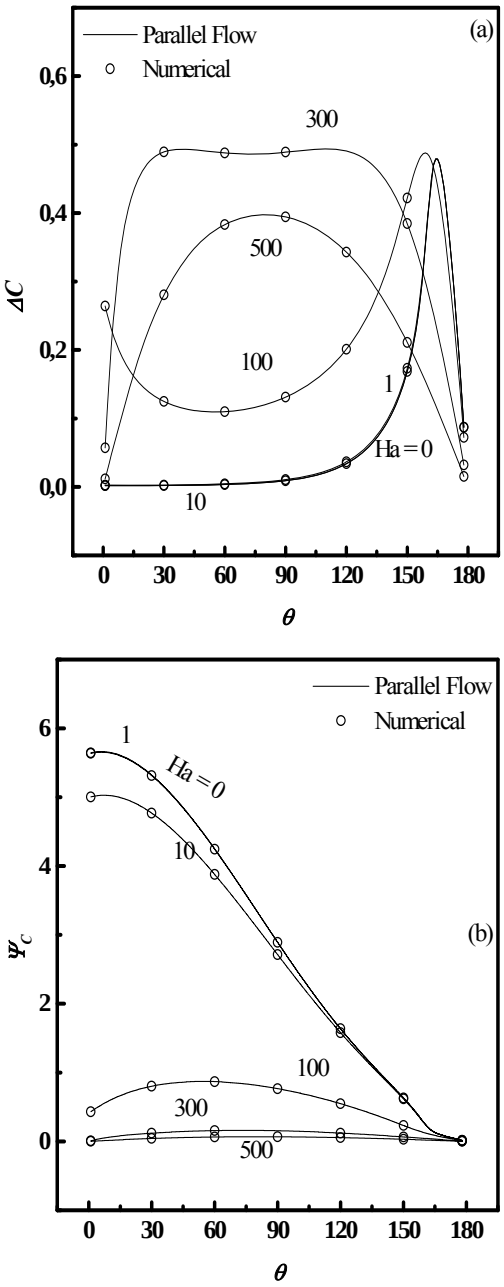

Fig. 9. Variations vs. θ of ΔC (a) and ψ_C (b) for $Le = 10$, $\varphi = 0.5$, $R_T = 10^5$, $Da = 10$ and various values of *Ha*.

$\theta\left(23^\circ \le \theta \le 130^\circ\right)$ with a very slight dip between these two limits leading to a relative minimum of ΔC barely observed around $\theta \approx 72^\circ$. Globally, in this range of θ, ΔC varies only by about 2% ($\Delta C_{min} \approx 0.48$ and $\Delta C_{max} \approx 0.49$). The effect of *Ha* on the flow intensity, exemplified in Fig. 9b could be determinant depending on the intensity of the magnetic field and the cavity inclination. The combined effect of *Ha* and θ is seen to offer the possibility to reach ΔC_{max} around 0.49 (the highest value attained) by bringing the flow intensity to the weaker required values ensuring the

optimum coupling between thermodiffusion and natural convection. Moreover, the importance of the results presented demonstrates the possibility to realize a good separation of species even for high Rayleigh numbers (for which experiments are more easily accessible compared to those attempted with feeble values of this parameter). This occurs by counter-acting the promoting effect of R_T on the flow intensity with damping effects realized by other parameters like Hartmann number and cavity inclination.

6. CONCLUSION

Effect of magnetic field on species separation based on the Soret driving convection in an inclined porous cavity saturated by an electrically conducting binary mixture and having impermeable boundaries to mass transfer, is studied analytically and numerically using the extended Darcy-Brinkman model. The study is mainly axed on porous and fluid media as limiting cases covered by the present study for small and high Darcy numbers, respectively. For a positive parameter of separation, illustrated $\varphi = 0.5$, the optimum conditions leading to the maximum separation of specifies are determined. For given R_T , Da and θ , the existence of specific values and/or ranges of Ha leading to maximize ΔC is confirmed. Particularly, for denser porous medium and $R_T = 200$, the important separation is produced for inclinations around 163° at relatively small *Ha*. However, at relatively large values of Ha but lower than some threshold beyond which the separation phenomenon vanishes, the maximum of separation requires an appropriate choice of the inclination in the range $\left[45^\circ - 150^\circ\right]$. Furthermore, the separation phenomenon is seen to be weakly affected when the inclination angle is varied in the range $\left[45^\circ - 150^\circ\right]$ for relatively small Ha . At high Ha , there exists wide ranges of θ within which important separation of species can be obtained. At small values of Ha , the separation of species is obtained only for specific inclinations depending on the Hartman number.

REFERENCES

Ahadi, A., T. Yousefi and M. Z. Saghir (2013). Double diffusive convection and thermodiffusion of fullerene–toluene nanofluid in a porous cavity. *The Canadian Journal of Chemical Engineering* 91(10), 1918-1927.

Alavyoon, F. (1993). On natural convection in vertical porous enclosures due to prescribed fluxes of heat and mass at the vertical boundaries. *International Journal of Heat Mass Transfer* 36, 2479-2498.

Amahmid, A., M. Hasnaoui, M. Mamou and P. Vasseur (1999). Double-diffusive parallel flow inducedin a horizontal Brinkman porous layer subjected to constant heat and mass fluxes: analytical and numerical studies. *Heat Mass Transfer* 35, 409-421.

Bennacer, R., A. A. Mohamad and M. El Ganaoui (2009). Thermosolutal diffusion in porous media: Multi-domainconstitutant separation. *International Journal of Heat and Mass Transfer* 52, 1725-1733.

Ben Sassi, M., S. Kaddeche, M. Lappa, S. Millet, D. Henry and H. Ben Hadid (2017). On the effect of thermodiffusion on solute segregation during the growth of semiconductor materials by the vertical Bridgman method. *Journal of Crystal Growth* 458, 154-165.

Bou-Ali, M. M., J. J. Valencia, J. A. Madariaga, C. Santamaria, O. Ecenarro and J. F. Dutrieux (2003). Determination of the thermosolutal diffusion coefficient in three binary organic liquid mixtures by the thermogravitational method. *Philosophical Magazine* 83(1718), 2011-2015.

Bourich, M. M. Hasnaoui, A. Amahmid and M. Mamou (2005). Onset of convection and finite amplitude flow due to Soret effect within a horizontal sparsely packed porous enclosure heated from below. *International Journal of Heat and Fluid Flow* 25, 513-525.

Clusius, K. and G. Dickel (1939). The separating tube process for liquids, *Naturwissenschaften* 27, 148-149.

Comarck, D. E., L. G. Leal and J. Imberger (1974). Natural convection in a shallow cavity with differencially heated end walls, Part 1: Asymptotic Theory. *Journal of Fluid Mechanics* 65, 209-230.

Costesèque, P. (1982). *Sur la migration sélective des isotopes et des éléments par la thermosolutale diffusion dans les solutions. Applications de l'effet thermogravitationnel en milieux poreux, observations expérimentales et conséquences géochimique.* Doctoral thesis, n° 1049, Université Paul Sabatier, Toulouse, France.

Costesèque, P., D. Fargue and Ph. Jamet (2002). Thermosolutal diffusion in porous media and its consequences. Thermal Non-equilibrium phenomena in Fluid Mixtures. *Lecture Notes in Physics, Springer, Berlin* 584, 389-427.

Costesèque, P., M. El Maâtaoui and E. Riviere (1994). Enrichissements sélectif d'hydrocarbures dans les huiles minérales naturelles par diffusion thermogravitationnelle en milieu poreux et cas des isomères paraffiniques. *Entropie* 184-185, 94-100.

De Groot and S. R. (1942). Théorie phénoménologique du procédé thermogravitationnel de séparation dans un liquide, *Physica* 9, 801-816.

Elhajjar, B., A. Mojtabi, P. Costesèque and M. C.

Charrier-Mojtabi (2010). Separation in an inclined porous thermogravitational cell. *International Journal of Heat and Mass Transfer* 53, 4844-4851.

Furry, W. H., R. C. Jones and L. Onsager (1939). On the theory of isotope separation by thermal diffusion. *Physical Review* 55, 1083-1095.

Larabi, M. A., D. Mutschler and A. Mojtabi (2016). Thermal gravitational separation of ternary mixture n-dodecane/ isobutylbenzene/ tetralin components in a porous medium. *Chinese Journal of Chemical Physics* 144, 244902/1-244902/7.

Jaber, T. J., M. Khawaja and M. Z. Saghir (2006). Permeability and Thermodiffusion Effect in a Porous Cavity Filled with Hydrocarbon Fluid Mixtures. *Fluid Dynamic and Material Processing* 2(4), 271-286.

Lorenz, M. and A. H. Emery (1959). The packed thermal diffusion column. *Chemical Engineering Science* 11, 16-23.

Marcoux, M. and P. Costesèque (2007). Study of transversal dimension influence on species separation in thermogravitational diffusion columns. *Journal of Non-Equilibrium Thermodynamics* 32, 289-298.

Martin-Mayor, A., M. M. Bou-Ali, M. Aginagalde and P. Urteaga (2018). Microfluidic separation processes using the thermodiffusion effect. *International Journal of Thermal Sciences* 124, 279-287.

Pal, D. and B. Talukdar (2012). Influence of Soret effect on MHD mixed convection oscillatory flow over a vertical surface in a porous medium with chemical reaction and thermal radiation. *International Journal of Nonlinear Science* 14, 65-78.

Platten, J. K. (2006). The Soret effect: A review of recent experimental results. *Journal of Applied Mechanics* 73, 5-15.

Platten, J. K., M. M. Bou-Ali, and J. F. Dutrieux (2003). Enhanced Molecular Separation in Inclined Thermogravitational Columns. *Journal of Physical Chemistry* B 107, 11763-11767.

Platten, J. K. and P. Costesèque (2004). The Soret coefficient in porous media. *Journal of Porous Media* 7, 329-342.

Raju, M. C., S. V. K. Varma, P.V. Reddy and S. Saha (2008). Soret effects due to natural convection between heated inclined plates with magnetic field. *Journal of Mechanical Engineering* 39, 65-70.

Rao, B. M. and G. V. Reddy (2012, July-August 2). Soret and Dufour effects on hydro magnetic heat and mass transfer over a vertical plate in a porous medium with a convective surface boundary condition and chemical reaction. *International Journal of Engineering Research and Applications* 4, 056-076.

Rtibi, A., M. Hasnaoui and A. Amahmid (2014). Magnetic field effect on Soret driving free convection in an inclined porous cavity saturated by a conducting binary mixture. International *Journal of Numerical Methods for Heat and Fluid Flow* 24 (8), 1715-1735.

Shevtsova, V. (2010). IVIDIL experiment on board the ISS. *Advances in Space Research* 46, 672–679.

Sprenger, L., A. Lange, S. Odenbach, (2013). Thermodiffusion in ferrofluids regarding thermomagnetic convection. *Comptes Rendus Mécanique* 341(4-5), 429-437.

Yacine, L., A. Mojtabi, R. Bennacer and A. Khouzam (2016). Soret-driven convection and separation of binary mixtures in a horizontal porous cavity submitted to cross heat fluxes. *International Journal of Thermal Sciences* 104, 29-38.